Eur. Phys. J. B **31**, 203–208 (2003)
DOI: 10.1140/epjb/e2003-00024-8

THE EUROPEAN PHYSICAL JOURNAL B

Carbon nanotube bundles and thin layers probed by micro-Raman spectroscopy

L. Sangaletti[1,a], S. Pagliara[1], F. Parmigiani[1], P. Galinetto[2], R. Larciprete[3], S. Lizzit[3], and A. Goldoni[3]

[1] Dipartimento di Matematica e Fisica and INFM, Università Cattolica, Via dei Musei 41, 25121 Brescia, Italy
[2] Dipartimento di Fisica "A. Volta" and INFM, Università di Pavia, Via Bassi 6, Pavia, Italy
[3] Sincrotrone Trieste, s.s. 14 Km 163,5 in Area Science Park, 34012 Trieste, Italy

Received 2 September 2002
Published online 4 February 2003 –

Abstract. Raman spectra of single-wall carbon nanotubes (CNTs) either in the form of micrometer sized bundles or thin layers prepared by dilution and sonication of powders have been compared. We have been able to collect the Raman spectrum of nanotube bundles that are not in touch with the substrate, and therefore not affected by interactions with the substrate surface. This spectrum resulted to be similar to that of the precursor nanotube powders, whereas relevant changes in the Raman spectrum are detected when the diluted powders form very thin layers on either metallic or insulating surfaces, as probed by confocal microraman imaging on well defined areas of the CNTs layers. In the case of thin layers, the intensity of the Raman D band, detected between 1 320 and 1 340 cm^{-1} and ascribed to disorder effects, is strongly enhanced. This enhancement occurs independently on the kind of substrate.

PACS. 73.63.Fg Nanotubes – 63.50.+x Vibrational states in disordered systems – 78.30.-j Infrared and Raman spectra

Introduction

A wide range of potential applications for carbon nanotubes (CNTs), assembled to fabricate electrical and mechanical nanodevices, has raised much interest on this nanostructured form of carbon. In the design of nanodevices, possible changes in the properties of CNTs at the interface between the CNT itself and other materials cannot be neglected. For example, for application of CNTs in electronic components, site-specific assemblies of nanotubes onto patterned substrates are required. This can be accomplished by surface modifications favoring the attachment of nanotubes to an electrode [1]. Indeed, a recent work shows that a deformation of adsorbed nanotubes due to the interaction with the surface may occur [2]. This finding has implications for electronic transport and tribological properties of adsorbed CNTs. The interest in these aspects of nanotube-substrate interaction is also large in view of the dramatic dependence of the electronic structure on the substrate material already observed for single layers of C_{60} and C_{70} fullerides, *i.e.*, the other nanostructured form of carbon [3].

Raman spectroscopy is one of the most used tools in the characterization of CNTs. Due to the high Raman cross section for the active vibrational modes and to the possibility to work at resonant excitation frequencies, Raman spectroscopy was recently shown to be a non-destructive probe for the investigation of nanotubes [4]. In principle, this probe is capable of determining the diameter and the electronic properties of single-wall CNTs. Moreover, when combined with a confocal microscope, the Raman probe can be integrated into a scanning confocal Raman imaging system which can provide a mapping of the Raman bands from a sample with a lateral resolution of about 1 μm. Mews *et al.* have carried out a Raman imaging study of individual bundles of nanotubes, by combining confocal Raman spectroscopy and AFM microscopy [5]. In this study it was possible to distinguish between the separate CNTs and to perform spatially resolved Raman spectroscopy within a given bundle of CNTs deposited onto a low-roughness Si_3N_4 membrane.

Many other experiments have been carried out with samples prepared in different ways, including deposition onto substrates for surface-enhanced Raman scattering (SERS) investigations [6–10]. Several layers have been prepared for SERS experiments on carbon CNTs. Corio *et al.* [6] have deposited silver or gold layers on glass to obtain clusters of metal particles. Colloidal silver clusters were used by Kneipp *et al.* [7,8]. Azoulay *et al.* have carried out SERS experiments on single hot-spot site [9] whereas Duesberg *et al.* [10] were able to perform polarized microraman spectroscopy on spatially separated single-wall CNTs.

[a] e-mail: sangalet@dmf.bs.unicatt.it

While all the previous studies have been carried out in the presence of a specific substrate, the Raman study of single-wall CNTs not interacting with the substrate has been so far virtually neglected. Only in a recent experiment, the electronic properties of self-standing CNTs bundles with a diameter of about 150 nm were mapped by photoemission spectro-microscopy [11].

The aim of the present study is to track changes in the Raman scattering of single-wall CNTs either in the form of micrometer sized bundles that are not in touch with any substrate (bridge-like CNTs), except for the bundle extremities, or thin layers deposited onto either metallic or insulating substrates. We have been able to collect the Raman spectrum of bridge-like bundles with a size down to one micrometer, prepared by dilution and sonication of powders. This spectrum results to be similar to that of the precursor powders, whereas relevant changes in the Raman spectrum are detected when the diluted powders form very thin layers onto either metallic or insulating surfaces. In the case of thin CNTs layers, the enhancement of the intensity of the band at about 1 330 cm^{-1} (usually denoted as D band in graphite) is related to defects in the graphene sheets or size effects as observed by Maurin *et al.* [12]. Moreover, this enhancement occurs independently on the kind of substrate and, therefore, in this case can not be ascribed to the chemical degradation induced at SERS conditions, invoked by Lefrant *et al.* to explain the dependence of the D band on the layer thickness [13].

Experiment

High quality purified single-wall CNT powder (by CARBOLEX [www.carbolex.com]), originally produced by laser vaporization of carbon with Ni/Co catalyst, was first sonically dispersed in toluene, then sonically dispersed in acetone and finally deposited, *via* evaporation of the solvent, on a clean copper grid or a copper platelet.

Microraman spectra from the nanotube powders were collected by a Dilor Labram spectrograph. The excitation source was a HeNe laser (632.8 nm; *i.e.* 1.96 eV) with a power of the order of 10 mW, focussed down to a diffraction limited spot size of about 1 micrometer. This set up yielded an excitation power of about 1MW/cm^2 on the sample. A Renishaw spectrograph was used to collect the Raman spectra with a photon energy of 2.41 eV (514 nm) obtained from an air-cooled Ar laser source. In both cases, a microscope was coupled confocally to the spectrograph. Rejection of the elastically scattered line was obtained with a holographic notch filter. The lateral resolution of the Labram probe during the microraman mapping was about 1 μm, resulting from the focussing of the laser beam with a 100x (N.A. = 0.9) microscope objective.

Results and discussion

In the following, the Raman spectra of the precursor powders are presented. From these powders, micrometer sized bundles and thin layers were obtained after deposition onto a metallic (copper) mesh or a copper platelet.

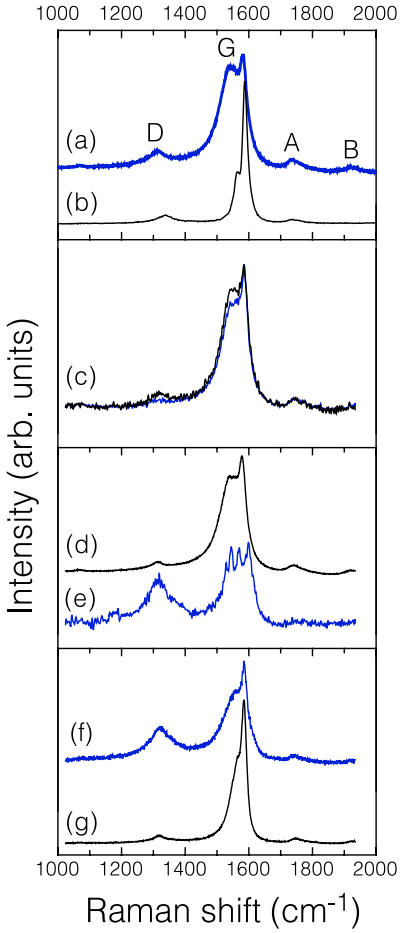

Fig. 1. Microraman spectra of the single-wall CNT collected under different preparation conditions. (a) Precursor powders, $\lambda = 632$ nm. (b) Precursor powders, $\lambda = 514$ nm. (c) representative Raman spectra collected from the bundle of Figure 2b. (d) Representative Raman spectrum collected from the CNT deposited onto the copper mesh (thick layer). (e) Representative Raman spectrum collected from the CNT deposited onto the copper mesh (very thin layer, not visible under the microscope). (f) Representative Raman spectrum collected from the CNT deposited onto the copper plate (thick layer). (g) Representative Raman spectrum collected from the CNT deposited onto the copper mesh (thin layer).

Figure 1 shows the Raman spectra collected with 632.8 nm (a) and 514.0 nm (b) laser sources in the 1 200–2 000 cm^{-1} range. In spectrum (a) several bands can be clearly detected at about 1 312 (D), 1 580 (G), 1 736 (A) and 1 920 (B) cm^{-1}. The wavenumber of D and G peaks increases with the photon energy, as reported in Table 1. These features are typical of Raman bands arising from single-wall CNTs [14]. Moreover the G-band at about 1 580 cm^{-1} is much broader when collected with 1.96 eV photon energy and displays a fine structure.

Table 1. Measured wavenumber of the Raman active modes detected with a laser excitation energy of 1.96 eV (He-Ne laser) and 2.41 eV (Ar^+ laser).

$h\nu$ (eV)	D (cm^{-1})	G (cm^{-1})	A (cm^{-1})	B (cm^{-1})
1.96	1 312	1 580	1 736	1 920
2.41	1 340	1 587	1 734	-

The Raman spectra of CNTs have been intensively studied both experimentally and theoretically [15]. The modes that are observed in Raman spectroscopy of CNTs fall into two distinct energy regions, the low energy region around 150–200 cm^{-1} and the high energy modes between 1 500–1600 cm^{-1}. The Raman bands detected in the low-energy region originate from a breathing-like vibration of the tube with strong van der Waals intertube contribution. The modes in this region are denoted as radial breathing modes (RBM). The frequency of the RBM mode was found to be inversely proportional to the radius of the tube and independent of the chiral angle [16,17]. The high-energy modes are usually related to a displacement pattern derived from the E_{2g} bond stretching mode of graphite.

Both the Raman bands of the high frequency tangential (1 500–1 600 cm^{-1}) and low-frequency (140–250 cm^{-1}) modes exhibit a strong resonant behavior. The spectrum of semiconducting tubes, excited with *e.g.* a blue laser line is dominated by two peaks at about 1 592 and 1 565 cm^{-1}, whereas the metallic nanotube spectra, enhanced by red excitation, extends down to 1 540 cm^{-1}. In fact, the CNTs can be metallic or semiconducting, depending on the magnitude and direction of its chiral vector. Usually, CNTs are found in bundles or ropes containing both semiconducting and metallic NT, which have different density of states and therefore resonate at different frequencies.

The intensity of the peak at 1 330 cm^{-1} may vary with respect to that of the band at 1 540–1 600 cm^{-1}. The appearance of peak D has been tentatively assigned to symmetry lowering effects such as defects of nanotube caps, bending of the nanotube, or the presence of nanoparticles and amorphous carbon (Ref. [15], Chap. 10). The A-peak at 1 735 cm^{-1} has been ascribed to second-order Raman processes involving combinations of radial and tangential modes. Peaks (B) at 1 920 cm^{-1} are also ascribed to second-order Raman processes.

In Figure 2a an image of the nanotubes deposited onto the copper mesh is shown. A micron sized bundle can be detected at the center of the figure. The enlargement of the region that includes the bundle is shown in Figure 2b. This bundle bridges one of the mesh wires (top of Fig. 2b) to an agglomerate of nanotubes (bottom-right corner of Fig. 2b). The microraman map of the area selected in Figure 2a is shown in Figure 2c. This map was taken by setting a 10×10 points grid onto the selected area. The gray scale represents the scattered intensity from the G band of the nanotube Raman spectrum: the darker the color, the

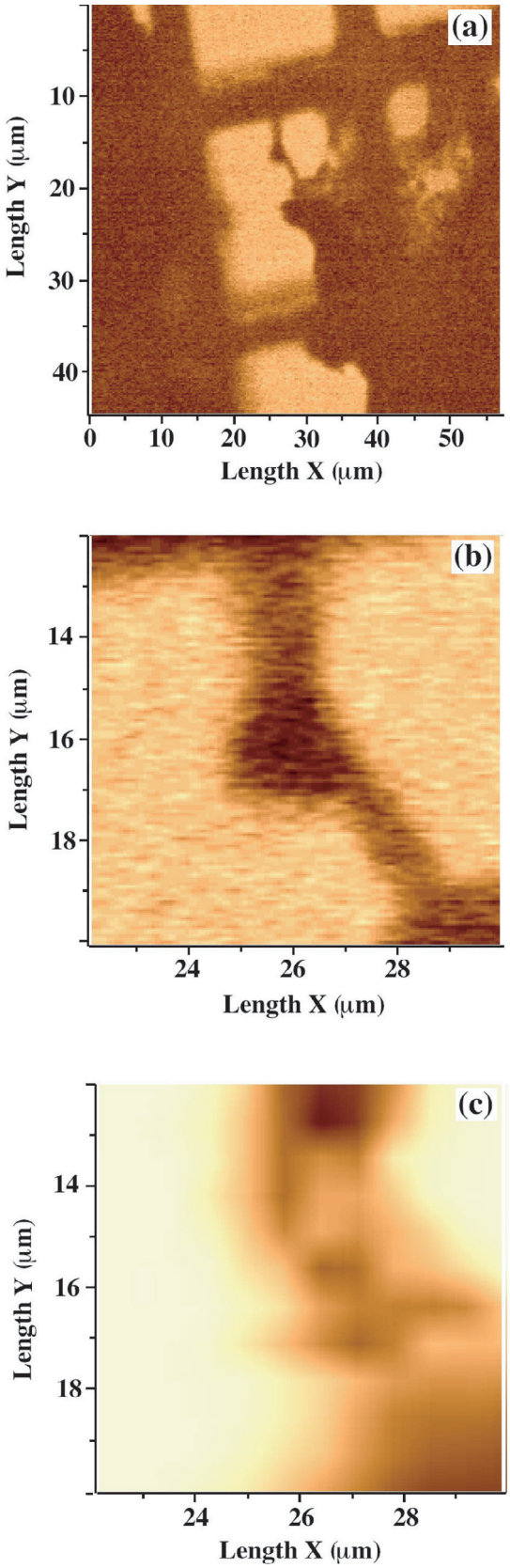

Fig. 2. (a) Optical image of the copper mesh with CNT aggregates. (b) Optical image of a free standing CNT bundle. (c) Microraman mapping of the G band intensity from the free standing bundle.

higher the scattered intensity. Taking into account the lateral resolution of the microraman probe, the dark region well matches the shape of the bundle evidenced in Figure 2b. In Figure 1c two representative spectra from the nanotube bundle are shown. They differ by slight intensity variations of the D band, as well as of the shoulder at low energy of the G band. Spectra from other points of the bundle are quite similar, with intensity differences within the variation presented in Figure 1c. Therefore, on the basis of these results we can conclude that the Raman spectrum of nanotubes from free standing aggregates bundles with a size down to about one micron is similar to that of the precursor, not diluted, powders. A better imaging resolution on free standing CNTs was only achieved with a photoemission micro-spectroscopy probe at the ELETTRA synchrotron light source in Trieste [11]. Instead, higher resolution imaging on CNT bundles were obtained from samples deposited onto substrates [5]. However, these experiments profited from the possibility to collect tapping-mode AFM images of the area of interest, which are not feasible for free standing objects. Therefore, the possibility to collect images of thinner free-standing bundles (*i.e.* tens of nanometers instead of the micrometer sized bundles studied in the present work) with confocal Raman imaging is still severely limited. Further developments may come from the use of Raman probes coupled with scanning near field optical microscopes.

The present results also enable us to discuss the role of SERS effect on the Raman investigation of CNTs. Kneipp *et al.* [7]. have shown a set of microraman spectra collected from a large bundle (10 μm diameter) of CNTs deposited onto a surface prepared for SERS with colloidal Ag clusters. These authors were able to detect a Raman signal only when the bundle was in touch with an Ag cluster. This is at odd with later results of Mews *et al.* [7], as well as with the present data where it is recognized that SERS effects are not required to have a well detectable emission from CNTs either from an insulating substrate or from free-standing bundles.

In order to probe the effect of substrates on thin layers of nanotubes, microraman maps were collected also from nanotube aggregates deposited onto the mesh copper wires (Fig. 3). In this case, a line scan along one of the wires covered by nanotube aggregates was carried out. Figure 3a shows the optical image of two crossing wires. On the wire running from the top-left down to the bottom-right corner the nanotube aggregate is clearly detectable. The dotted line shows the points from which the Raman spectra were collected. The surface plot of Figure 3b shows the result from the line scan. On the x-axis the wave number is displayed, whereas spectra from the 50 probed points are stacked along the y-axis to yield the surface plot. The bright vertical region corresponds to the intensity of the G band. This intensity can vary considerably, but the overall features of most of the points are quite similar to the representative spectrum shown in Figure 1d. Only few spectra resulted to be different from that displayed in Figure 1d. These spectra are collected from regions were no aggregates are expected from an inspection of the optical image. However, when the microscope objective is pointed on these regions (*e.g.* the bright topmost region of the scan in Fig. 3a), quite different spectra are collected, such as that shown in Figure 1e. In this spectrum two bands are clearly detectable, which correspond to D and G bands of Figure 1a. The G band presents a fine structure with a sequence of four peaks. Similar results were obtained by Duesberg *et al.* [18] when single-wall CNT species deposited onto colloidal silver were observed by Raman spectroscopy. These authors reported several spectra with C-C stretching modes in the 1 510–1 595 cm^{-1} wavenumber range, fitted by four Lorentzians. These well resolved features were detected from CNTs deposited onto SERS substrates. In particular, the four distinct bands were found to occur only for the CNTs which displayed a single RBM at low wavenumbers. Moreover, in these spectra also an intense peak al 1 270 cm^{-1} (D band) was observed and tentatively ascribed to a selective surface enhancement of the Raman modes.

The present data do not allow us to draw a conclusion on this point. We have not systematically observed this feature and a more extensive study is required to clarify this problem.

Figures 3c–d shows the results of the mapping of Raman bands of CNTs deposited onto a copper substrate by dilution and sonication of powders. Figure 3c shows the optical microscope image (collected with a 100X objective) of the sampled area. In the darker area a higher concentration of CNTs is present, which absorb the laser light, whereas in the brighter area, due to the low CNT coverage, the light of the microscope illuminator is reflected from the copper substrate. In Figures 1f–g two representative Raman spectra are shown. One of them (Fig. 1f) was taken from the brighter area (more diluted CNT layer) whereas the other spectrum (Fig. 1g) was taken from the darker area. The main difference between these spectra is the intensity ratio between the disorder related D band and the G bands. In spectrum of Figure 1f the D/G intensity ratio is enhanced with respect to the spectrum shown in Figure 1g. When this intensity ratio is mapped onto the sampled area, the image shown in Figure 3d is obtained. The darker areas represent higher values of the D/G ratio, which correspond to the bright region of Figure 3c, where a thinner layer was is found. Therefore, there is a close correspondence between disorder effects, obtained for diluted layers, and the intensity of the D band in the Raman spectra. Quite a similar behavior was also observed in CNTs layers deposited onto insulating substrates (alumina or glass) [19]. Therefore the increase of the intensity of the D band can be related to disorder effects, and not to the insulating or metallic nature of the substrate. This finding poses several questions on the origin of the disorder-related D band. In a recent work Lefrant *et al.* [13] have claimed that surface chemical effects lead to the appearance of disorder in thin nanotube films. In this view, because of the physico-chemical interactions with the metallic substrate prepared for SERS experiments, graphite-like particles such as highly oriented pyrolytic graphite, carbon nanoparticles either close to amorphous

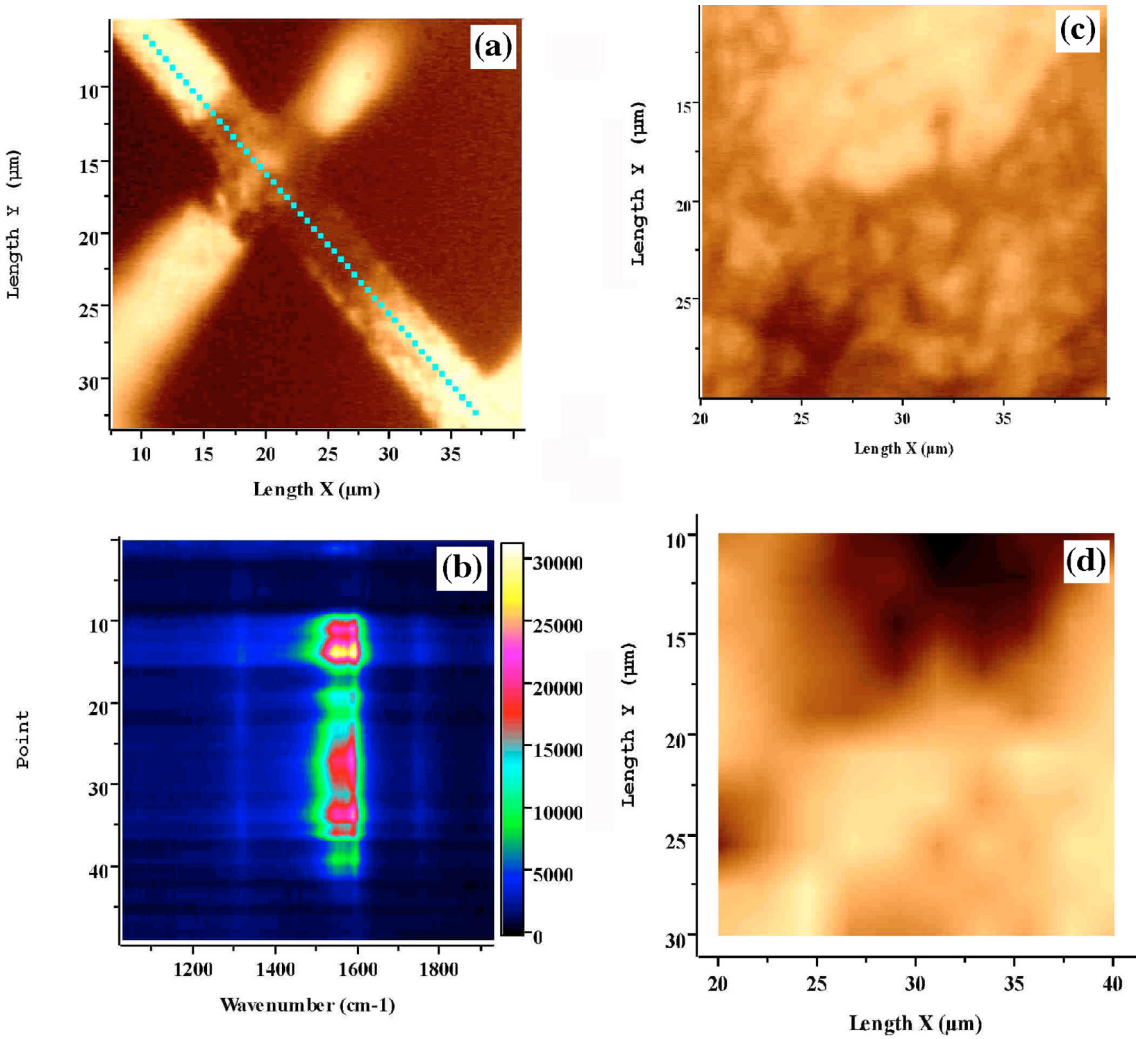

Fig. 3. (a) Optical image of one of the wires of the copper mesh with CNT aggregates. (b) Microraman mapping of the G band intensity along the wire. (c) Optical image of CNT aggregates deposited onto a copper plate. (d) Microraman mapping of the D/G intensity ratio of the CNT aggregates deposited onto the copper plate.

carbon or precursor of the closed shell fullerenes are expected. Our result points out that the degradation occurring at SERS conditions is not the only cause for the appearance of disorder and that for CNTs layers with reduced thickness –prepared also on insulating substrates– a large amount of disorder is already present, which increases the intensity of the Raman D band. Moreover, the similar behavior observed for layers deposited onto metallic and insulating substrates is not surprising. Indeed, a metallic substrate does not necessarily produce SERS effect unless it is properly prepared for the experiment, *e.g.* by etching the surface to yield a considerable roughness.

Our results also show that disorder can be inhomogeneously distributed within the same layer and this distribution corresponds to an inhomogeneous distribution of the thickness. This makes microraman confocal imaging a necessary tool to discriminate the contribution from different microscopic regions to the overall spectrum collected from a CNTs sample.

In conclusion, Raman spectra of single-wall carbon nanotubes either in the form of micrometer sized bundles or thin layers prepared by dilution and sonication of powders have been collected and compared. Our aim was to explore possible changes in the Raman spectrum of CNTs, depending on the interaction with the substrate. We have been able to measure the Raman spectrum of nanotube bundles that are not in touch with the substrate, and therefore not affected by interactions with the substrate surface. This spectrum results to be similar to that of the powders. Also in the case of thick layers on metallic substrates, the Raman spectrum is very close to that observed for the powders. Relevant changes in the Raman spectrum are detected only when the diluted powders form very thin layers both on insulating or metallic surfaces. In the case of thin layers, the Raman band at 1 320–1 340 cm^{-1}, ascribed to confinement or disorder is strongly enhanced. This enhancement occurs independently of the kind of substrate and therefore is not ascribed to physico-chemical interactions with the substrate.

Support from the Centro Grandi Strumenti at the University of Pavia is acknowledged for the experiments with the DILOR confocal microraman imaging probe. F. Giorgis is acknowledged for the assistance during the microraman experiments with the RENISHAW probe. This work was partly financed by Sincrotrone Trieste under the project "Pristine and doped fullerene and carbon nanotubes".

References

1. M. Burghard, G. Duesberg, G. Philipp, J. Muster, S. Roth, Adv. Mat. **10**, 584 (1998)
2. T. Hertel, R.E. Walkup, P. Avouris, Phys. Rev. B **58**, 13870 (1998)
3. C. Cepek, A. Goldoni, S. Modesti, Phys. Rev. B **53**, 7466 (1996), P. Rudolf, in *Fullerenes and Fullerene Nanostructures*, edited by J. Fink, M. Mehring, S. Roth, Vol. 263 (World Scientific, Singapore, 1996); A. Goldoni, C. Cepek, E. Magnano, A.D. Laine, S. Vandre, M. Sancrotti, Phys. Rev. B **58**, 2228 (1998); A.J. Maxwell, P.A. Brühwiler, D. Arvanitis, J. Hasselström, M.K.-J. Johansson, N. Mårtensson, Phys. Rev. B **57**, 7312 (1998); B.W. Hoogenboom, R. Hesper, L. Tjeng, G.A. Sawatzky, Phys. Rev. B **57**, 11939 (1998)
4. A.M. Rao, E. Richter, S. Bandow, B. Chase, P.C. Eklund, K.W. Williams, M. Menon, K.R. Subbaswamy, A. Thess, R.E. Smalley, G. Dresselhaus, M.S. Dresselhaus, Science **275**, 187 (1997)
5. A. Mews, F. Koberling, T. Basché, G. Phillipp, G.S. Duesberg, S. Roth, M. Burghard, Adv. Mat. **12**, 1210 (2000)
6. P. Corio, S.D.M. Brown, A. Marucci, M.A. Pimenta, K. Kneipp, G. Dresselhaus, M.S. Dresselhaus, Phys. Rev. B **61**, 13202 (2000)
7. K. Kneipp, H. Kneipp, P. Corio, S.D.M. Brown, K. Shafer, J. Motz, L.T. Perelman, E.B. Hanlon, A. Marucci, G. Dresselhaus, M.S. Dresselhaus, Phys. Rev. Lett. **84**, 3470 (2000)
8. K. Kneipp, L.T. Perelman, H. Kneipp, V. Backman, A. Jorio, G. Dresselhaus, M.S. Dresselhaus, Phys. Rev. B **63**, 193411 (2001)
9. J. Azoulay, A. Debarre, A. Richard, P. Tchenio, S. Bandow, S. Iijma, Chem. Phys. Lett. **331**, 347 (2000)
10. G.S. Duesberg, I. Loa, M. Burhhard, K. Syassen, S. Roth, Phys. Rev. Lett. **85**, 5436 (2000)
11. A. Goldoni, R. Larciprete, L. Gregoratti, B. Kaulich, M. Kiskinova, Y. Zhang, H. Dai, L. Sangaletti, F. Parmigiani, Applied Phys. Lett. **80**, 2165 (2002)
12. G. Maurin, I. Stepanek, P. Bernier, J.-F. Colomer, J.B. Nagy, F. Henn, Carbon **39**, 1273 (2001)
13. S. Lefrant, I. Baltog, M. Baibarac, J. Schreiber, O. Chauvet, Phys. Rev. B **65**, 235401 (2002)
14. C. Thomsen, Phys. Rev. B **61**, 4542 (2000)
15. R. Saito, G. Dresselhaus, M.S. Dresselhaus, *Physical Properties of Carbon Nanotubes* (Imperial College Press, London 1998), Chapts. 9 and 10
16. S. Bandow, S. Asaka, Y. Saito, A.M. Rao, L. Grigorian, E. Richter, P.C. Eklund. Phys. Rev. Lett. **80**, 3779 (1998)
17. V.N. Popov, V.E. Van Doren, M. Balkanski, Phys. Rev. B **59**, 8355 (1999)
18. G.S. Duesberg, W.J. Blau, H.J. Byrne, J. Muster, M. Burghard, S. Roth, Chem. Phys. Lett. **310**, 8 (1999)
19. L. Sangaletti, unpublished results